Supporting Information

Tuning the Förster Overlap Integral: Energy Transfer over 20 Angstroms from a Pyrene-based Donor to Borondipyrromethene (Bodipy)

Dan Bai, Andrew C. Benniston, Jerry Hagon, Helge Lemmetyinen, Nikolai V. Tkachenko and Ross W. Harrington

Contents

S17. Top: Transient absorption profiles recorded after excitation of **PTTBD** in MeCN with a 70 fs laser pulse delivered at 400 nm. Time delays are shown. Bottom: Kinetic traces at two different probe wavelengths and the least-squares fit to the data points (red).

S18.Component differential absorption spectra recorded for **PTTBD** in toluene following excitation with a 70 fs laser pulse delivered at 400 nm. Time delays are shown.

S19.Component differential absorption spectra recorded for **PTTBD** in THF following excitation with a 70 fs laser pulse delivered at 400 nm. Time delays are shown.

S20.Component differential absorption spectra recorded for **PTTBD** in Et_2O following excitation with a 70 fs laser pulse delivered at 400 nm. Time delays are shown.

S21.Component differential absorption spectra recorded for **PTTBD** in methoxybenzene following excitation with a 70 fs laser pulse delivered at 400 nm. Time delays are shown.

S22.Component differential absorption spectra recorded for **PTTBD** in MeCN following excitation with a 70 fs laser pulse delivered at 400 nm. Time delays are shown.

S23.Component differential absorption spectra recorded for **PTTBD** in DCE following excitation with a 70 fs laser pulse delivered at 400 nm. Time delays are shown.

S24.Component differential absorption spectra recorded for **PTTBD** in cyclohexane following excitation with a 70 fs laser pulse delivered at 400 nm. Time delays are shown.

S25. Variation of the ratio of the rate for energy transfer and the radiative rate of the donor versus the overlap integral.

S26. Apparent "inverse" relationship between k_{EET} and $1/n^4$ for low polarity solvents (▲) and high polarity solvents (●).

Table S1. Values for measured rates of energy transfer and solvent parameters.

Table S2. Calculated parameters using the Förster equation assuming $\kappa 2 = 2/3$ and intramolecular distances R.

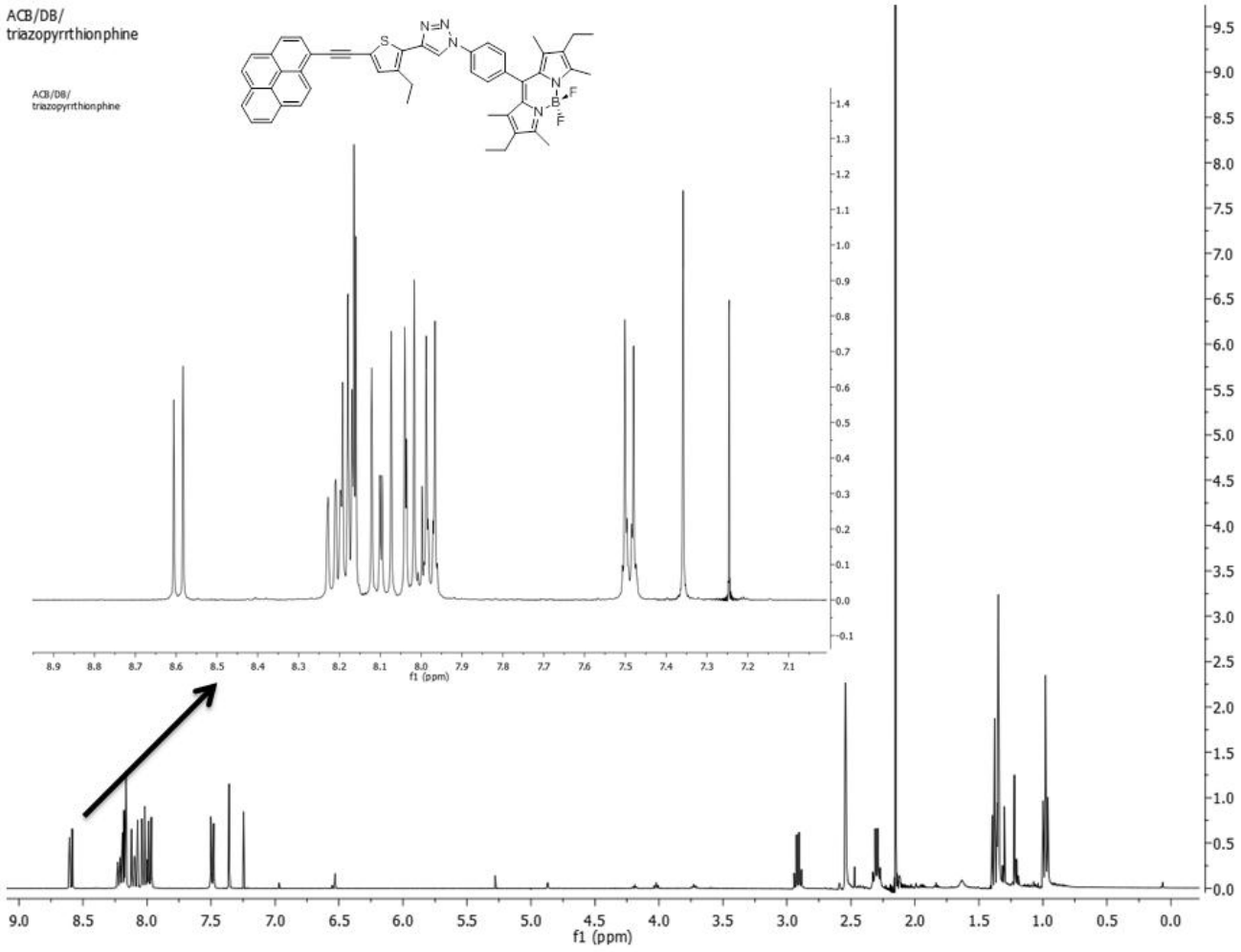

S1. Room temperature ^{1}H NMR spectrum for **PTTBD** in $CDCl_3$. Insert shows the expansion of the aromatic region and the sharp proton resonances.

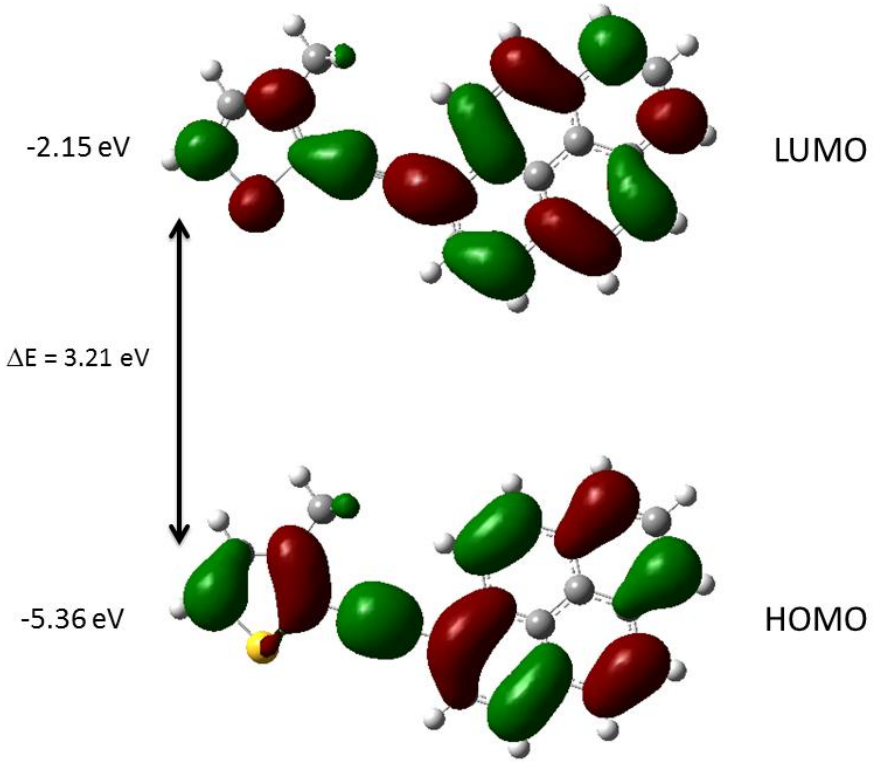

S2. Selected molecular orbitals calculated for **PT** using Gaussian 03 and DFT (B3LYP) and the 6-311G basis set. Energy given in eV.

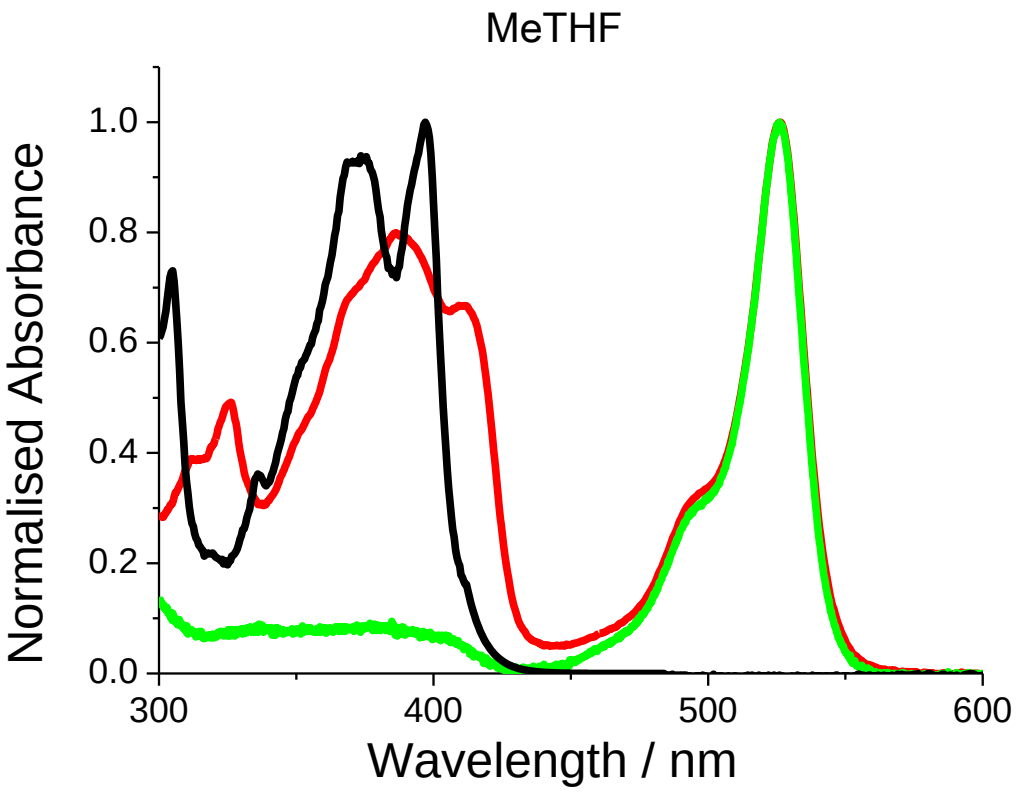

S3. Normalised room temperature absorption profiles recorded for **PT** (black), **BD** (green) and **PTTBD** (red) in MeTHF. Note: The small differences seen between **PT** and **PTTBD** for the pyrene-thiophene segment are a result of the triazole group which slightly perturbs the electronics of the system.

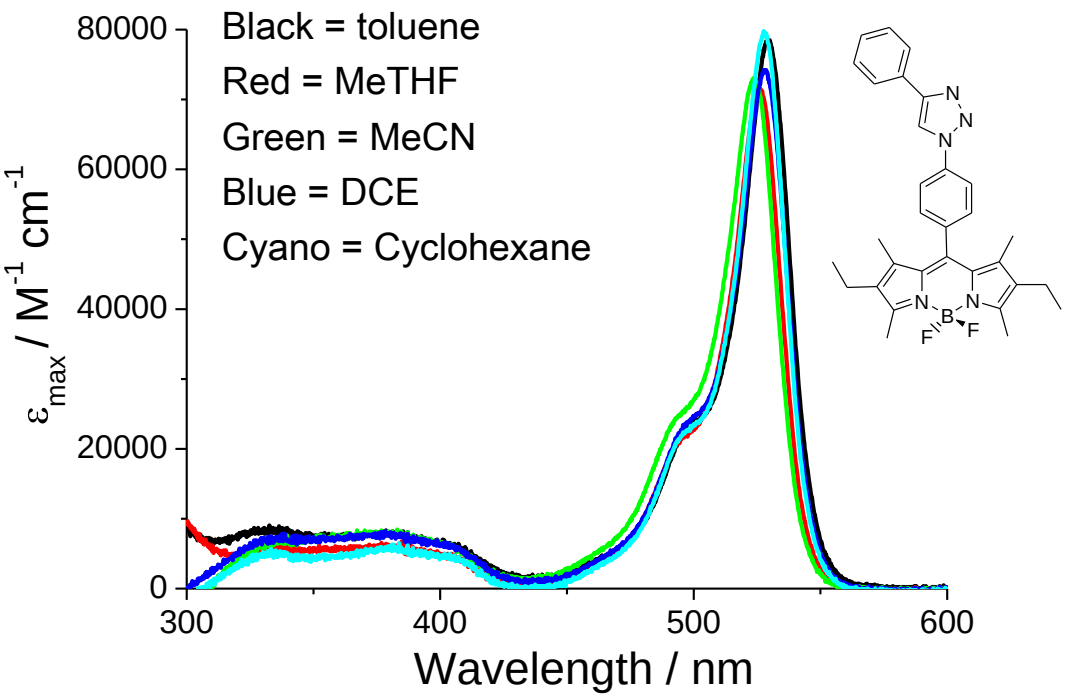

Table

Solvent	ε_{MAX} M^{-1} cm^{-1}
Toluene	78,500
MeTHF	72,000
MeCN	72,900
DCE	73,850
Cyclohexane	79,550

S4. Absorption spectra for **BD** in a range of solvents.

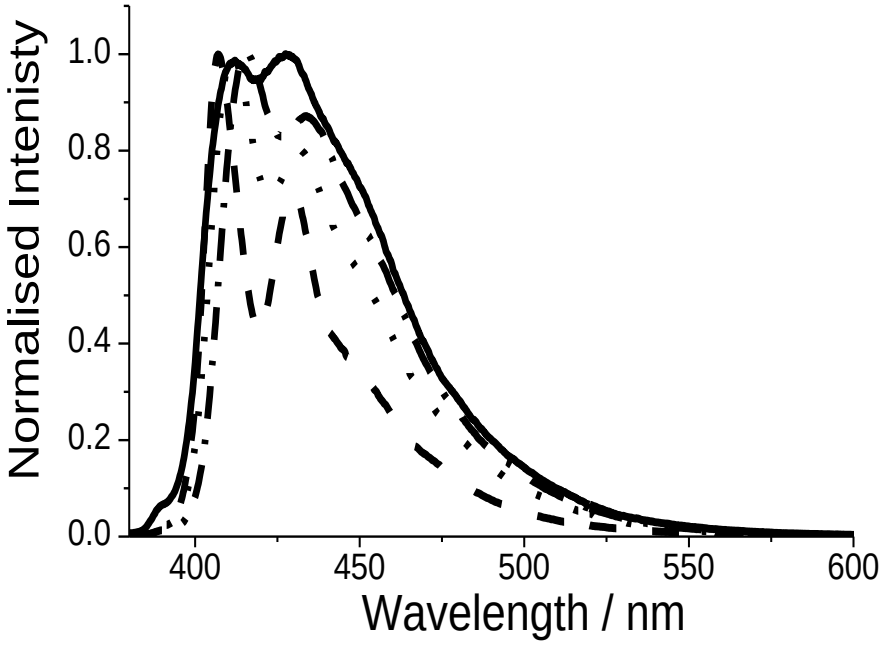

S5. Normalised fluorescence profiles recorded for **PT** in MeCN (black), CHX (dash), MeTHF (dot) and DCE (dash dot). Abbreviations defined in the main text.

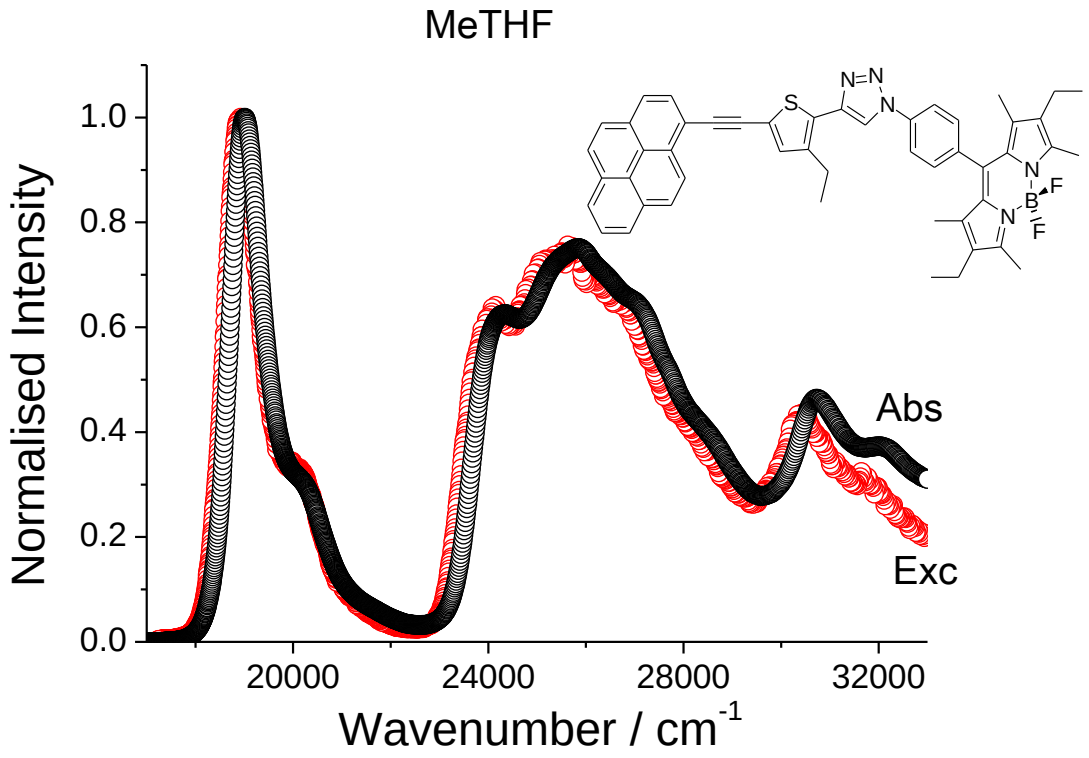

S6. Normalised absorption (black) and corrected fluorescence excitation spectrum (red) for **PTTBD** in MeTHF.

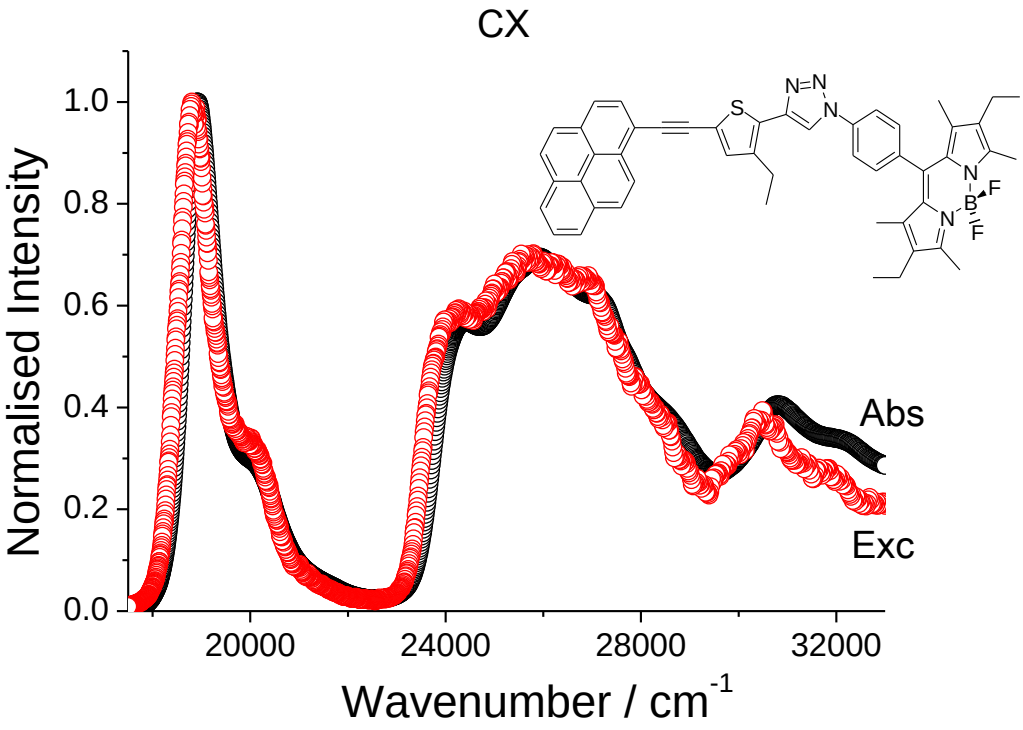

S7. Normalised absorption (black) and corrected fluorescence excitation spectrum (red) for **PTTBD** in cyclohexane.

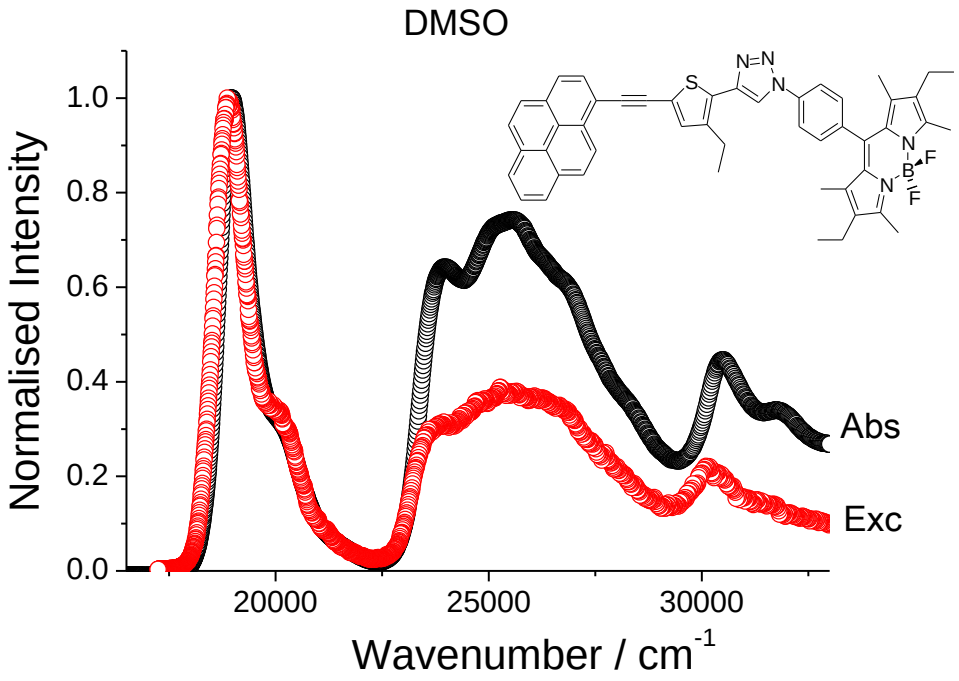

S8. Normalised absorption (black) and corrected fluorescence excitation spectrum (red) for **PTTBD** in DMSO.

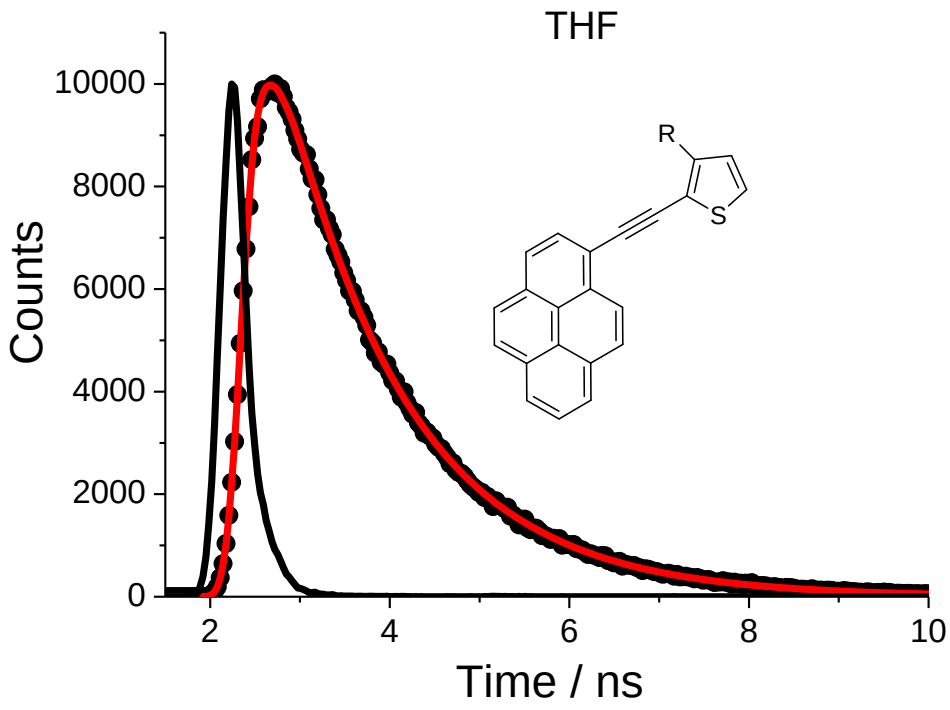

S9. Time-correlated single photon counting profile recorded for **PT** in THF showing the least-sqaures fit (red line) and instrument response function .

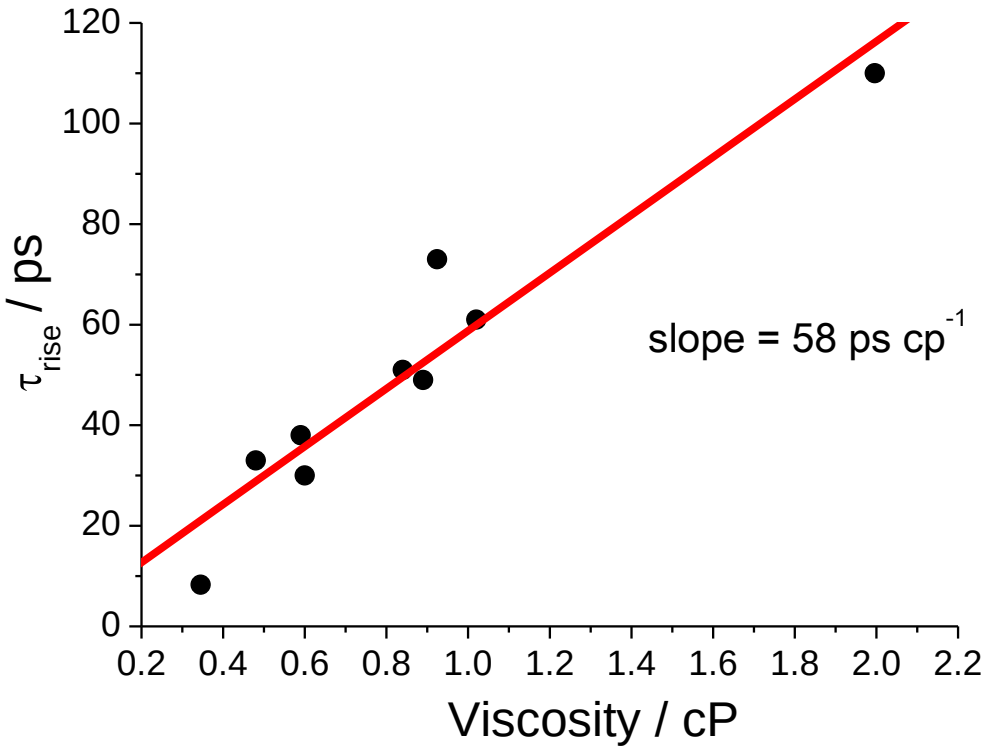

S10. Plot for the rise-time (τ_{RIS}) for the single-photon-counting data with the solvent viscosity. Red line represents the least-squares fit to the data points.

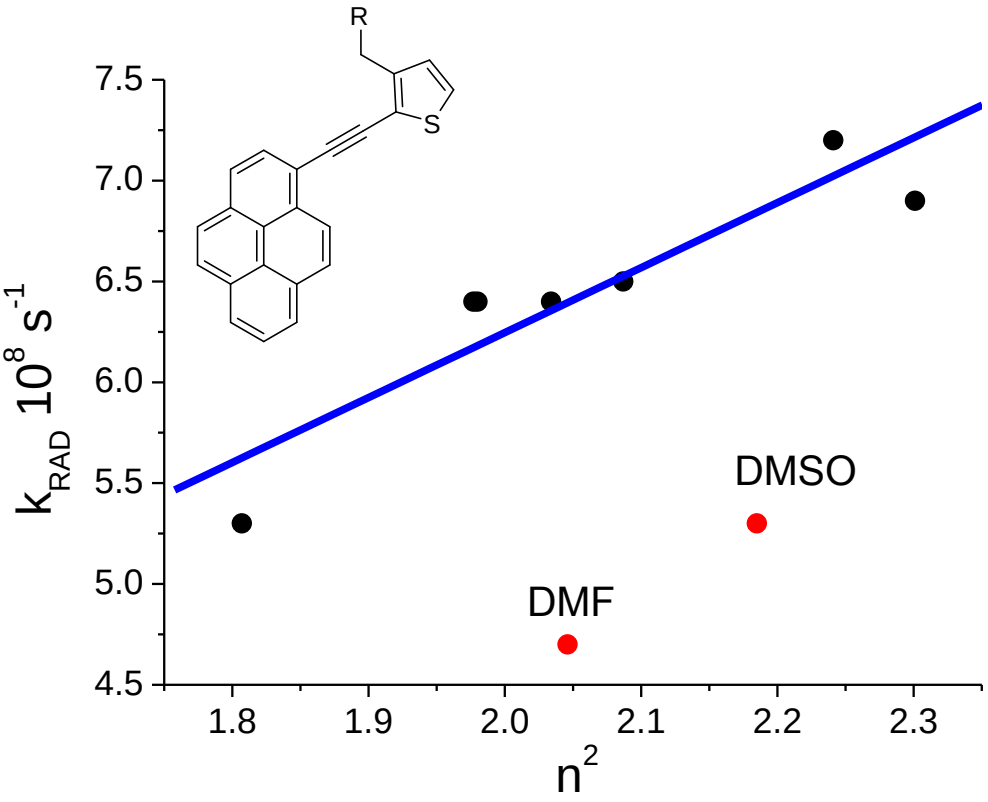

S11. Plot for the radiative rate constant (k_{RAD}) versus n^2 for **PT** in a range of solvents. Blue line represents the least-squares fit to the data points (●). The two anomalous data points are shown (●).

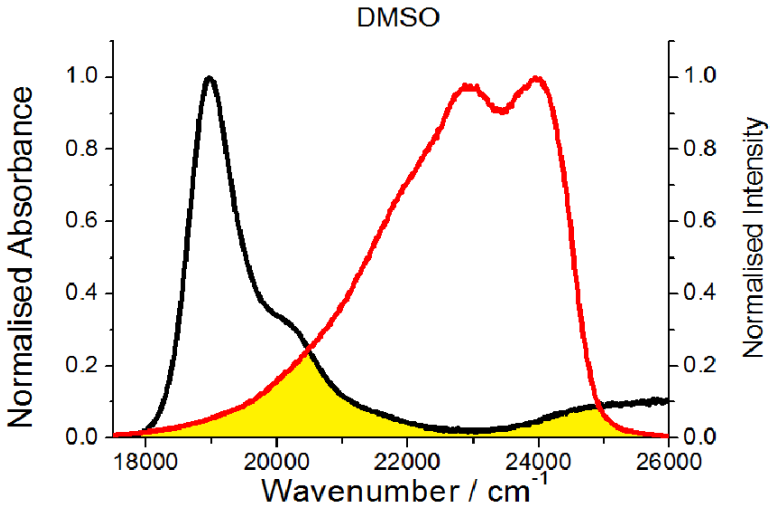

S12. The spectral overlap regions (yellow) from the normalised emission for **PT** and absorption for **BD** in DMSO.

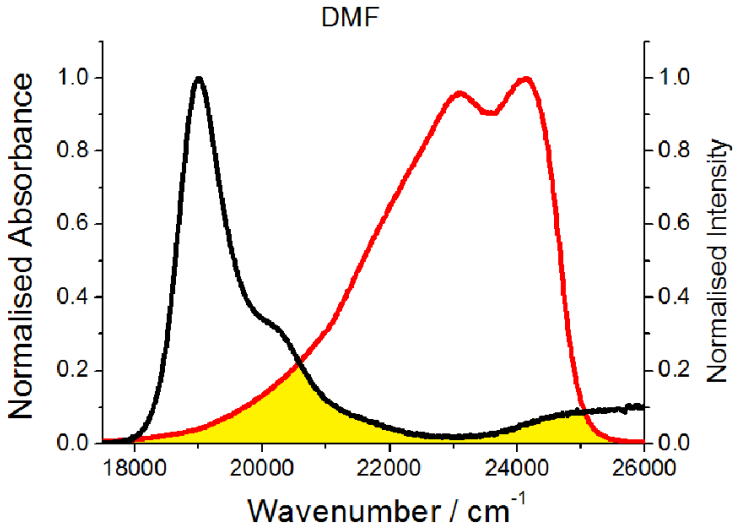

S13. The spectral overlap regions (yellow) from the normalised emission for **PT** and absorption for **BD** in DMF.

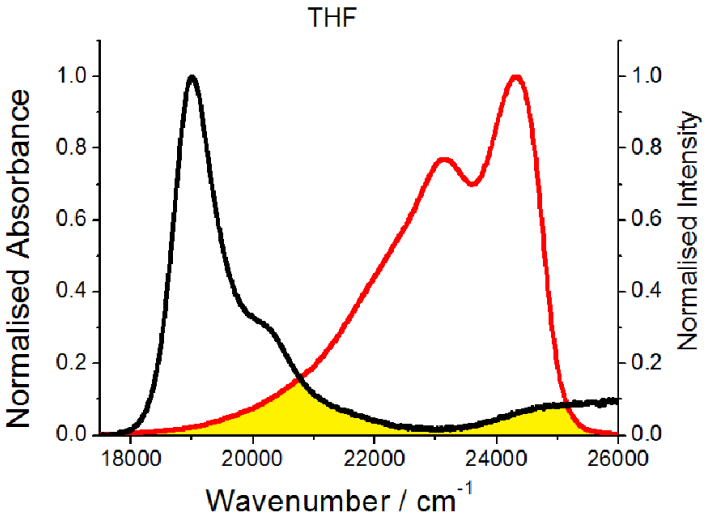

S14. The spectral overlap regions (yellow) from the normalised emission for **PT** and absorption for **BD** in THF.

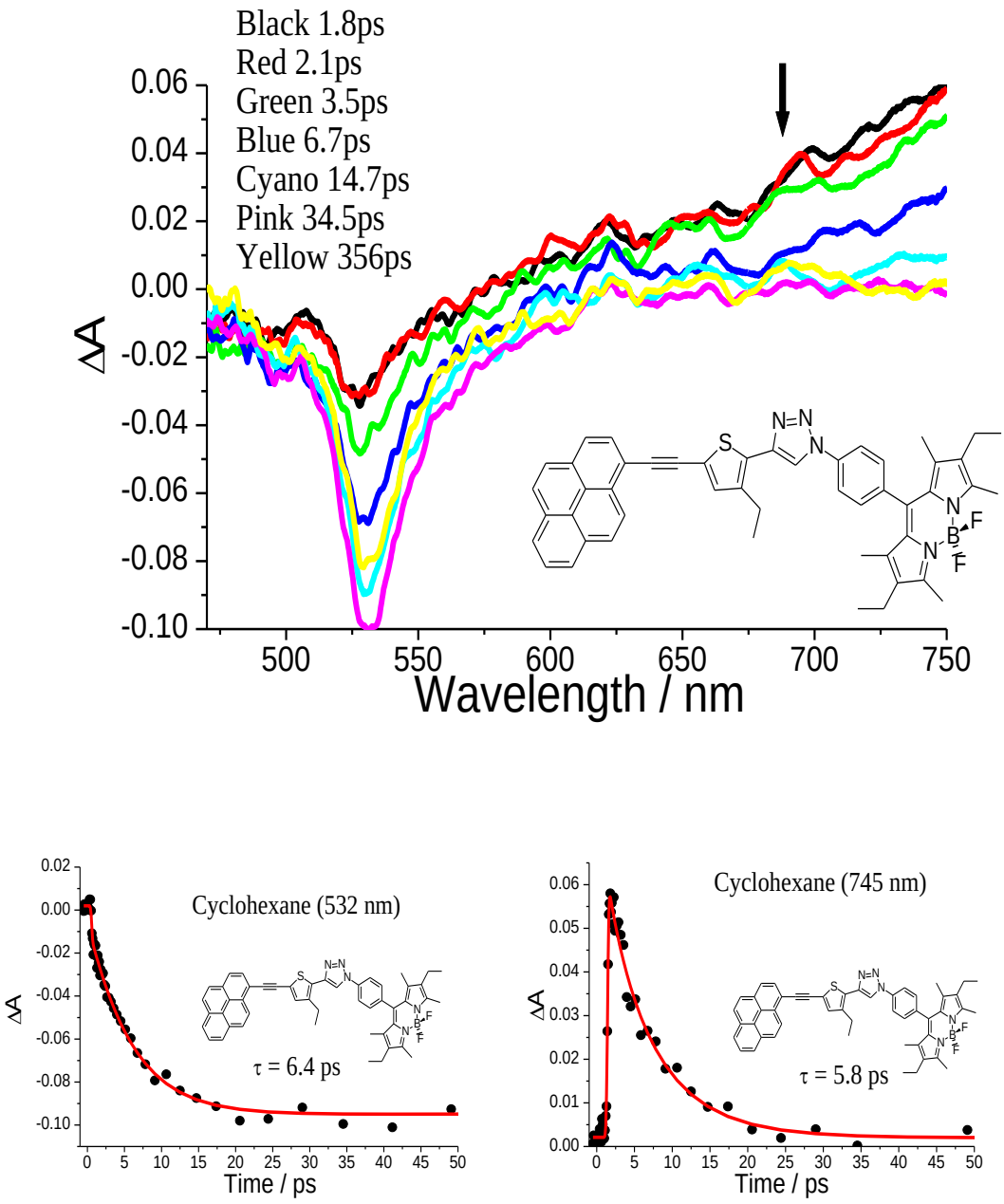

S15. Top: Transient absorption profiles recorded after excitation of **PTTBD** in CHX with a 70 fs laser pulse delivered at 400 nm. Time delays are shown. Bottom: Kinetic traces at two different probe wavelengths and the least-squares fit to the data points (red).

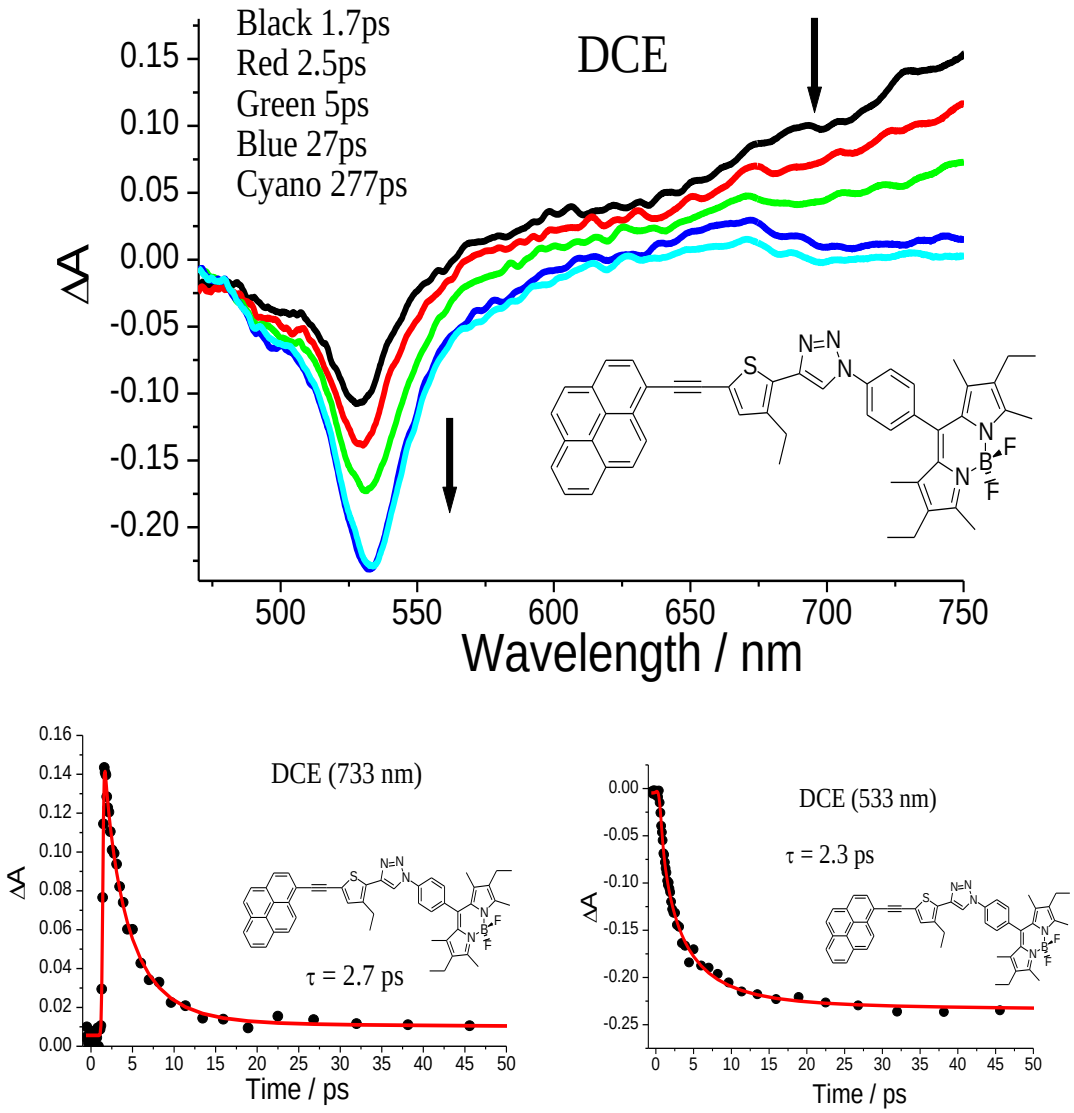

S16. Top: Transient absorption profiles recorded after excitation of **PTTBD** in DCE with a 70 fs laser pulse delivered at 400 nm. Time delays are shown. Bottom: Kinetic traces at two different probe wavelengths and the least-squares fit to the data points (red).

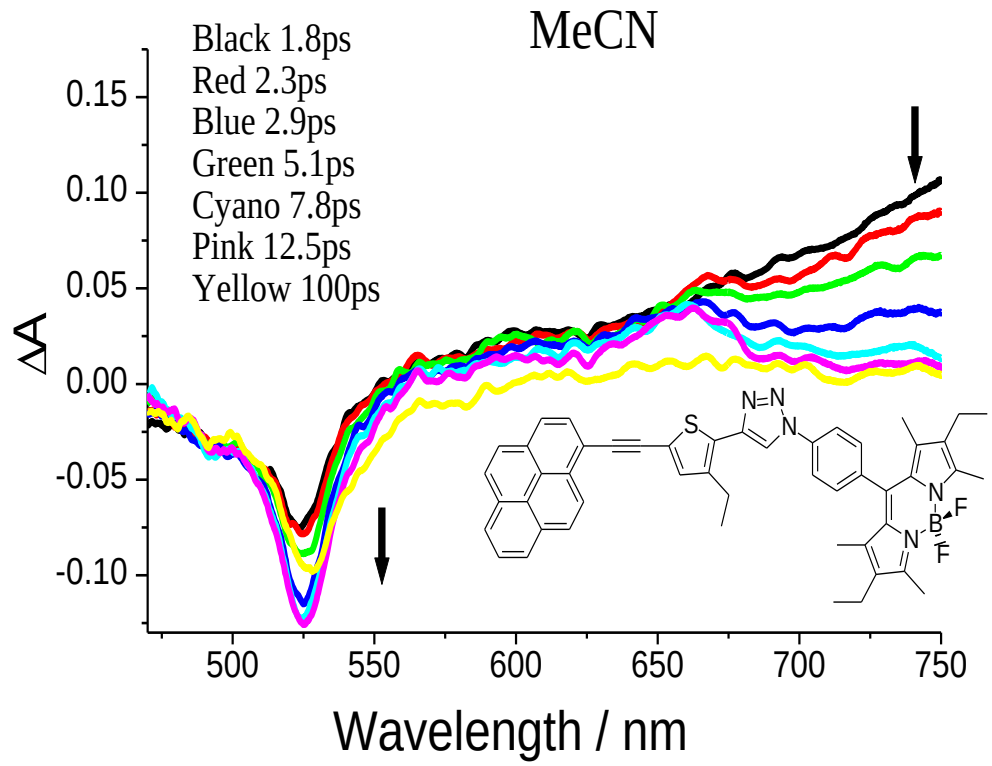

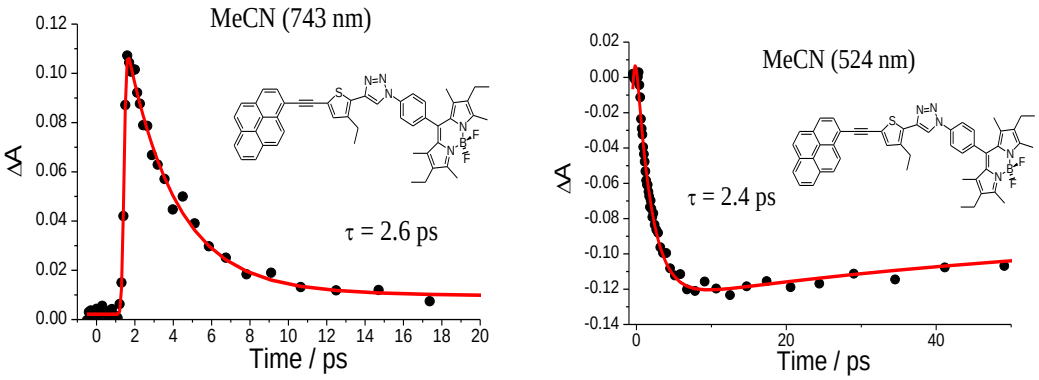

S17. Top: Transient absorption profiles recorded after excitation of **PTTBD** in MeCN with a 70 fs laser pulse delivered at 400 nm. Time delays are shown. Bottom: Kinetic traces at two different probe wavelengths and the least-squares fit to the data points (red).

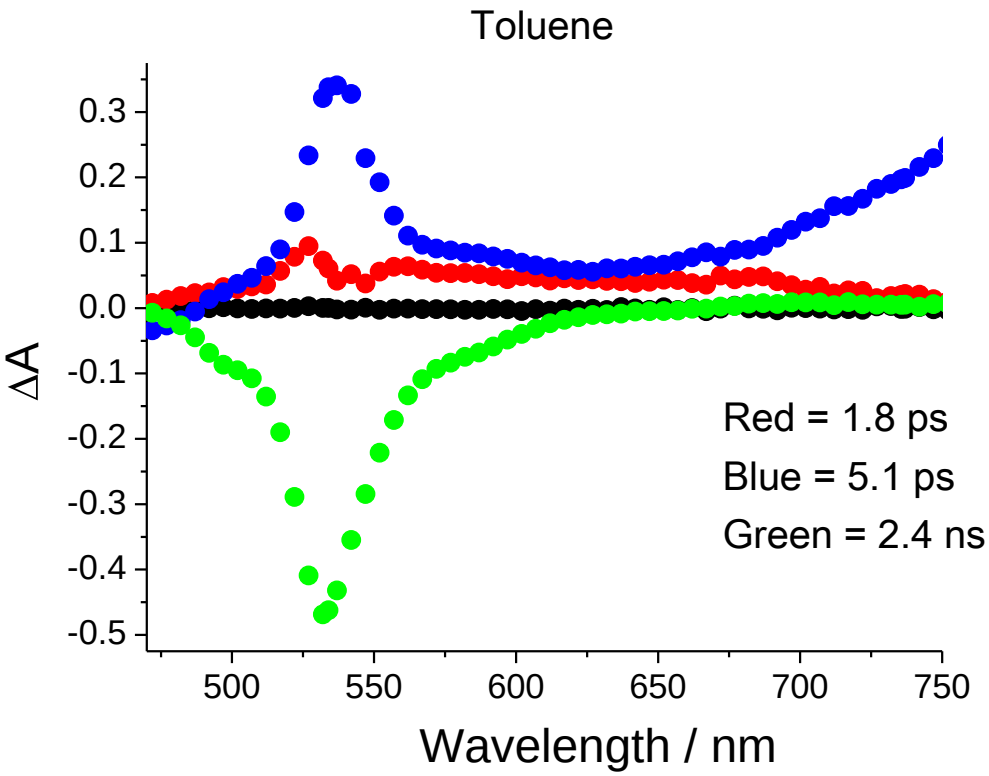

S18.Component differential absorption spectra recorded for **PTTBD** in toluene following excitation with a 70 fs laser pulse delivered at 400 nm. Time delays are shown.

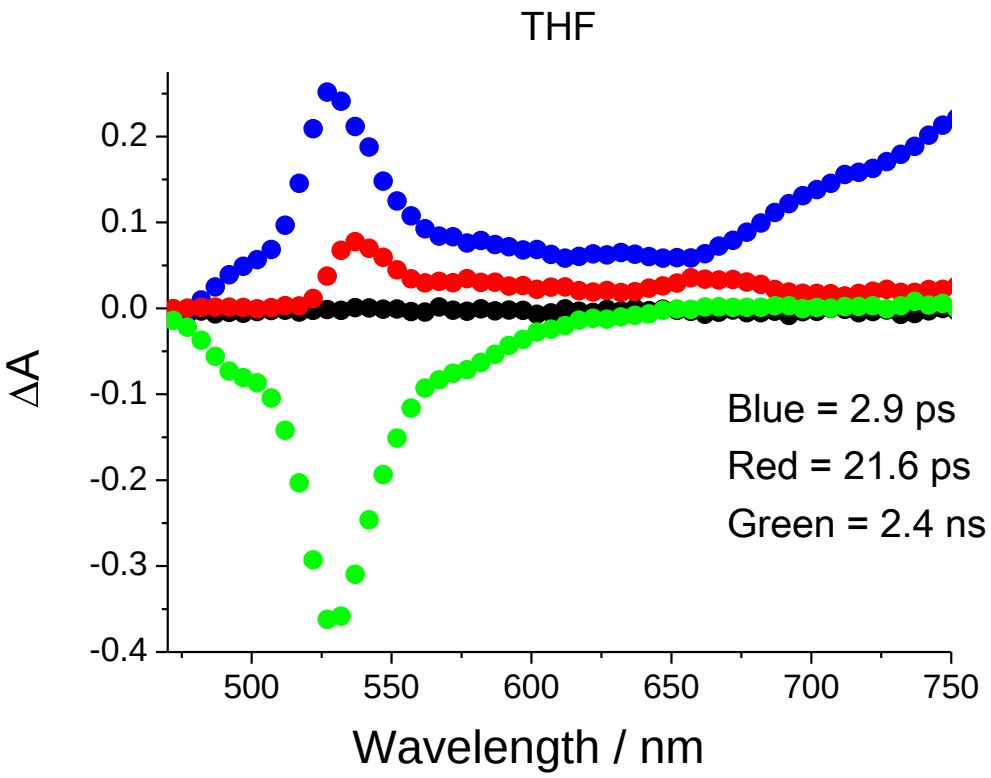

S19.Component differential absorption spectra recorded for **PTTBD** in THF following excitation with a 70 fs laser pulse delivered at 400 nm. Time delays are shown.

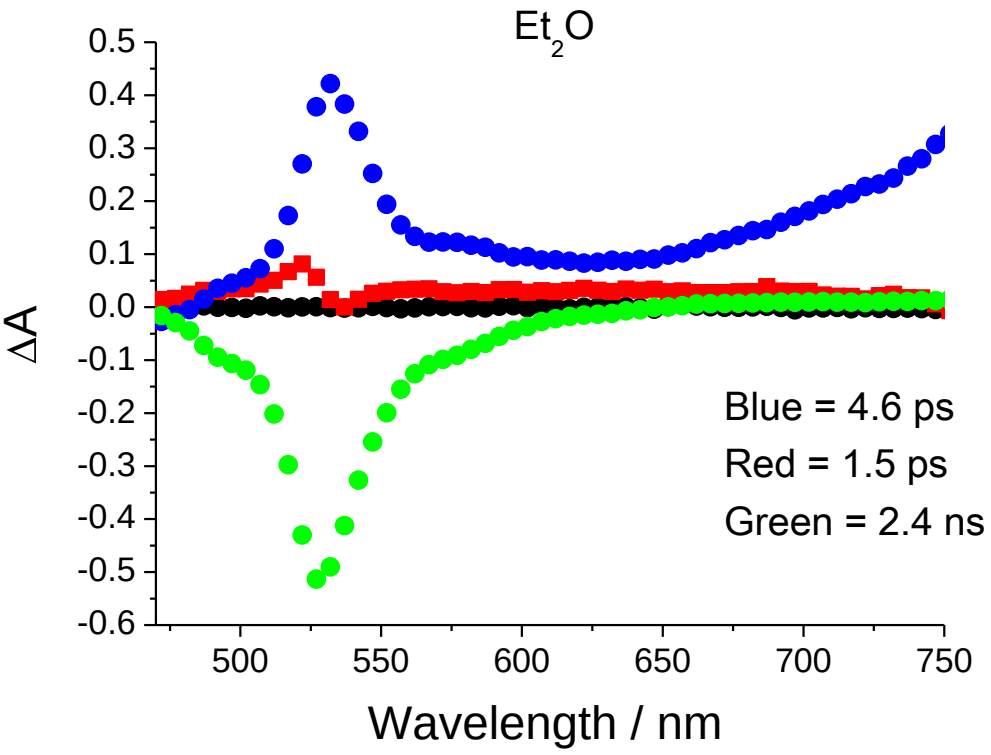

S20.Component differential absorption spectra recorded for **PTTBD** in Et_2O following excitation with a 70 fs laser pulse delivered at 400 nm. Time delays are shown.

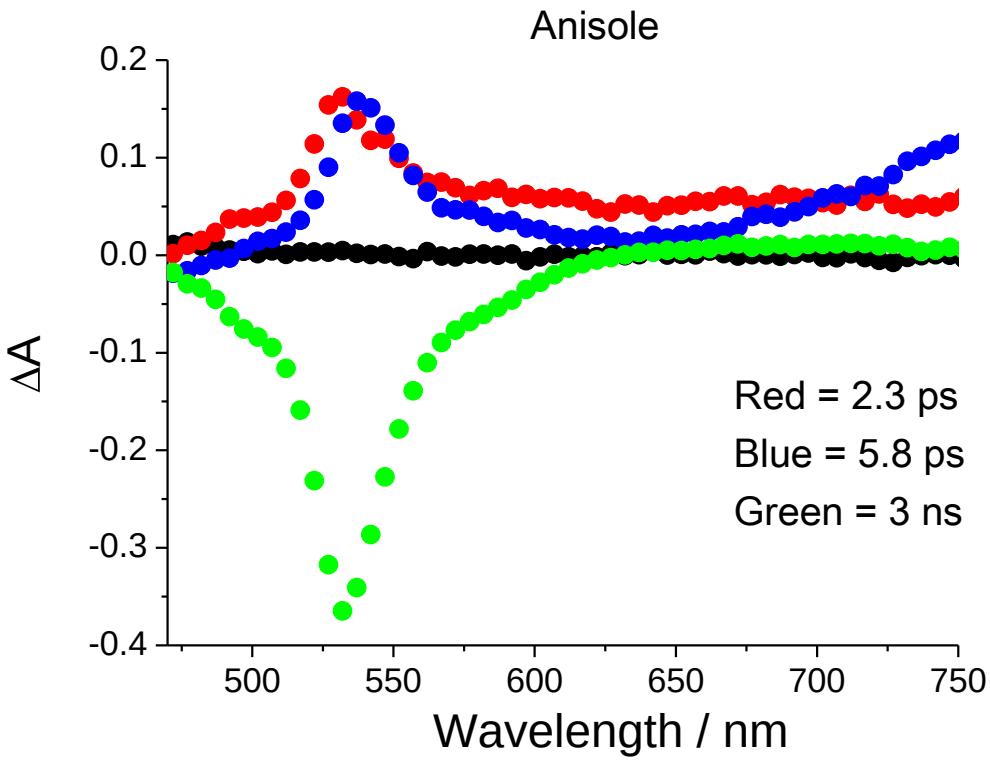

S21.Component differential absorption spectra recorded for **PTTBD** in anisole following excitation with a 70 fs laser pulse delivered at 400 nm. Time delays are shown.

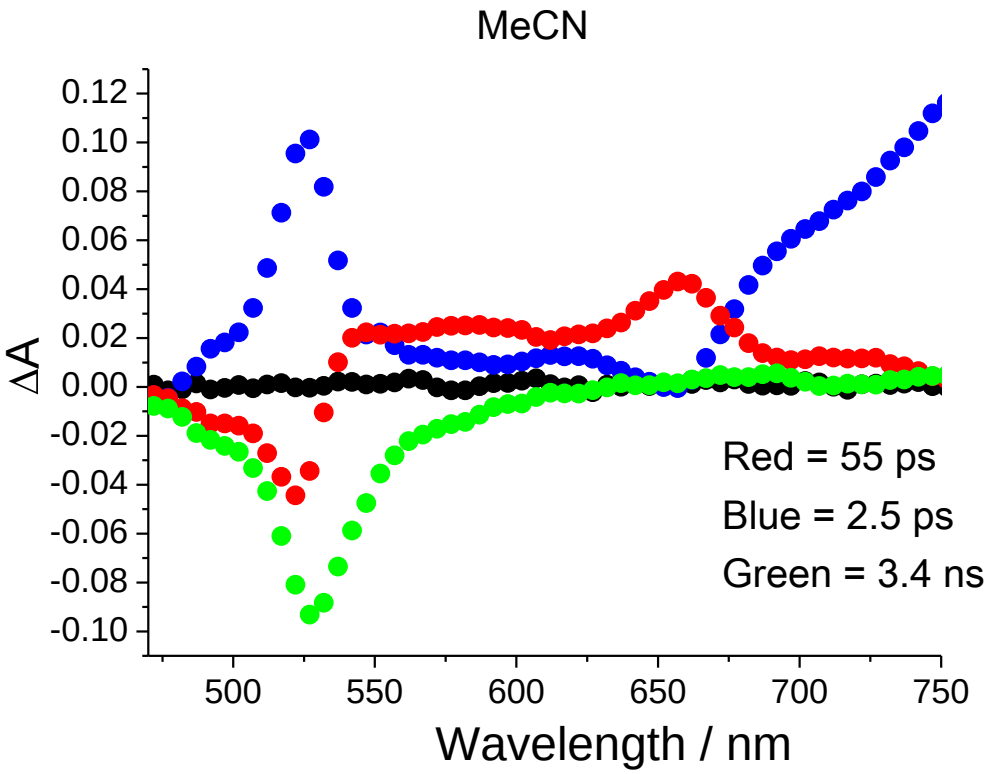

S22.Component differential absorption spectra recorded for **PTTBD** in MeCN following excitation with a 70 fs laser pulse delivered at 400 nm. Time delays are shown.

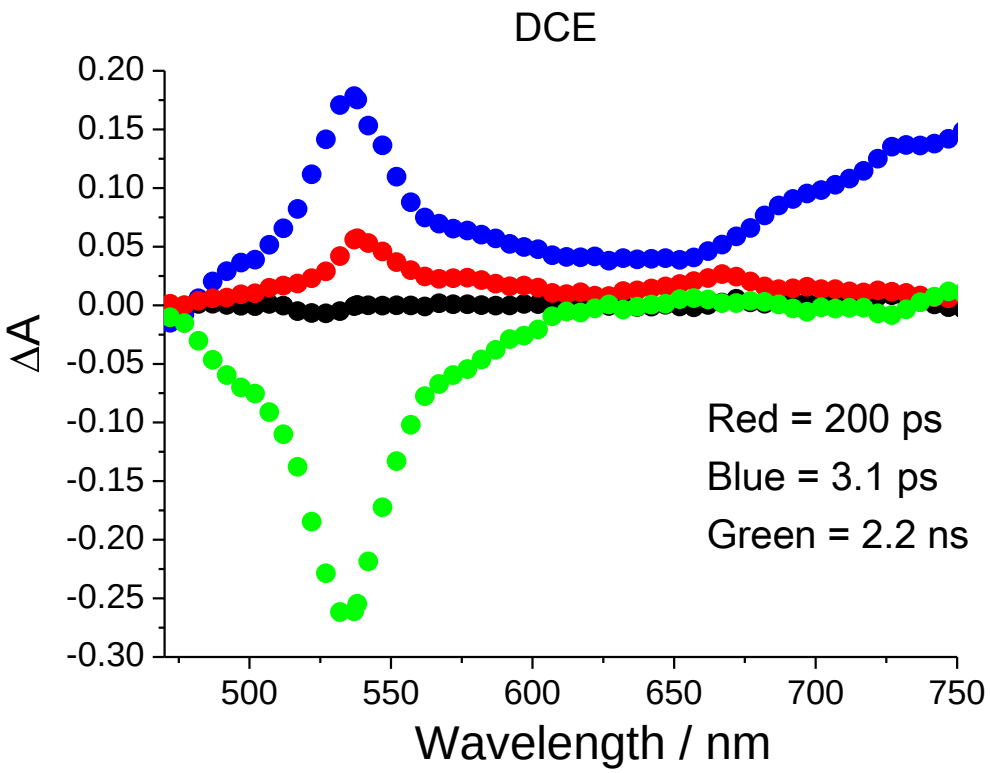

S23.Component differential absorption spectra recorded for **PTTBD** in DCE following excitation with a 70 fs laser pulse delivered at 400 nm. Time delays are shown.

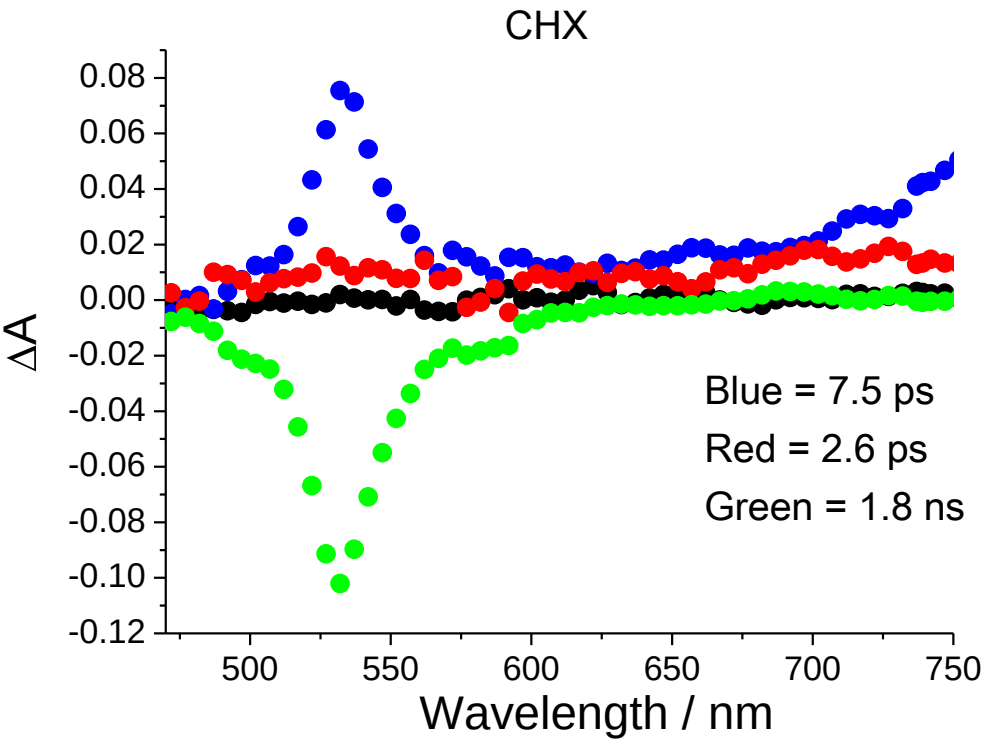

S24.Component differential absorption spectra recorded for **PTTBD** in cyclohexane following excitation with a 70 fs laser pulse delivered at 400 nm. Time delays are shown.

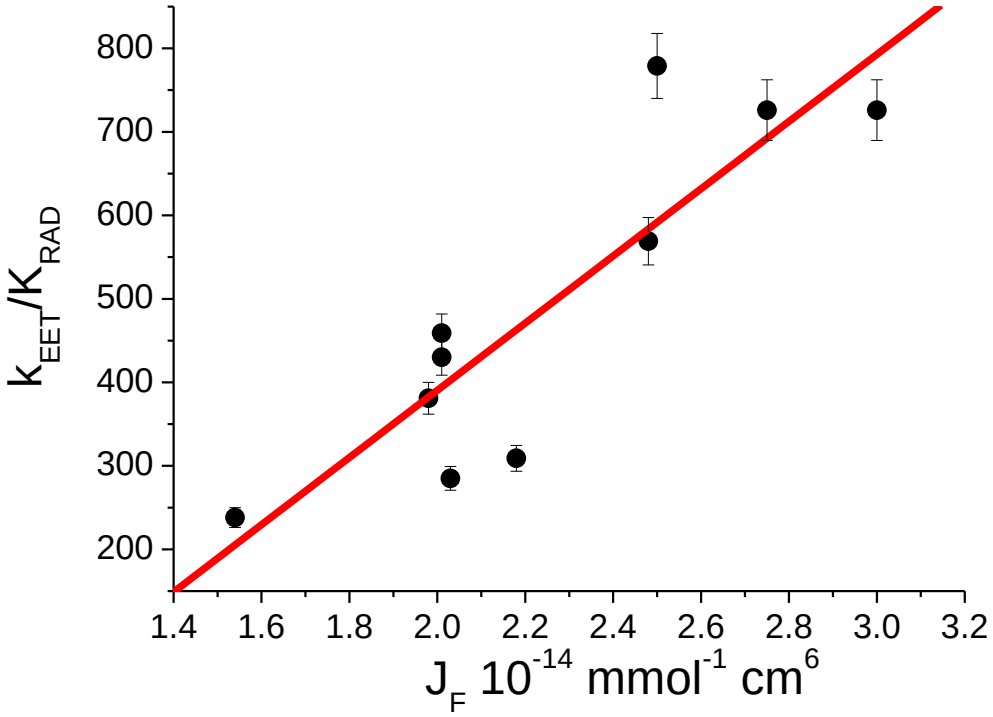

S25. Variation of the ratio of the rate for energy transfer and the radiative rate of the donor versus the overlap integral. Values for k_{RAD} are taken from S10.

Table S1. Values for measured rates of energy transfer and solvent parameters.

Solvent	k_{EET} 10^{11} / s^{-1} [a]	k_{EET}/k_{RAD}	n	$1/n^4$	ΔF[b]
MEB	2.13	309	1.517	0.189	0.112
MeTHF	2.75	430	1.403	0.258	0.203
DCE	3.70	569	1.445	0.229	0.221
CHX	1.52	238	1.426	0.242	~0
TOL	2.05	285	1.497	0.199	0.013
THF	2.94	459	1.407	0.255	0.210
DEE	2.17	381	1.352	0.299	0.167
DMF	3.66	779	1.430	0.239	0.274
DMSO	3.85	726	1.478	0.209	0.263
MeCN	3.85	726	1.344	0.306	0.307

[a]Average value. [b] Pekar function (see below)

$$\Delta F = \left(\frac{\varepsilon_s - 1}{2\varepsilon_s + 1}\right) - \left(\frac{n^2 - 1}{2n^2 + 1}\right)$$

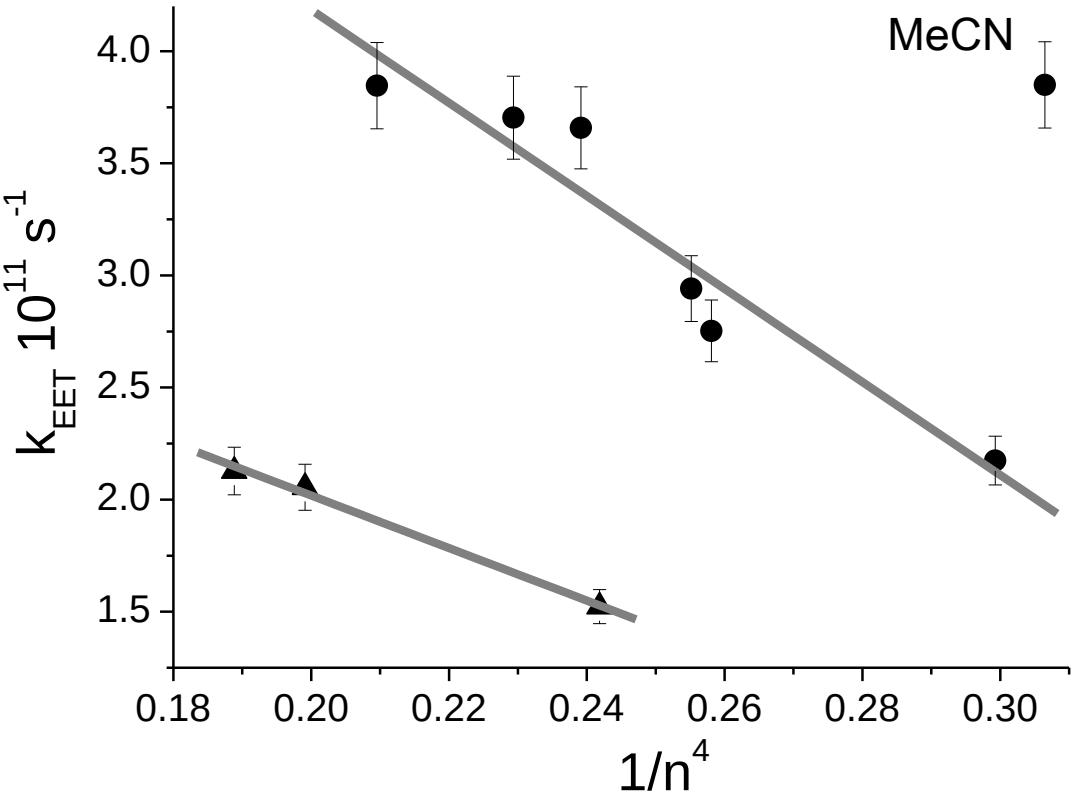

S26. Apparent "inverse" relationship between k_{EET} and $1/n^4$ for low polarity solvents (▲) and high polarity solvents (●).

Table S2. Calculated parameters using the Förster equation assuming κ^2 = 2/3 and intramolecular distances R as shown in Figure 1 below.[a]

Solvent	R_o / Å[b]	$k_{EET} / 10^{11}$ s^{-1}[c]	$k_{EET} / 10^{11}$ s^{-1}[d]	$k_{EET} / 10^{11}$ s^{-1}[e]	R / Å[f]
MEB	35.8	5.8	0.26	1.0	14.3
MeTHF	37.2	6.7	0.30	1.2	13.9
DCE	37.6	7.4	0.33	1.3	13.4
CHX	35.5	4.8	0.20	0.84	14.5
TOL	35.9	5.9	0.26	1.0	14.2
DMF	35.7	5.7	0.25	0.99	12.9
DMSO	36.4	6.8	0.30	1.2	13.1
THF	37.1	6.6	0.29	1.1	13.7
DEE	37.5	6.8	0.30	1.2	14.5
MeCN	39.2	9.0	0.40	1.6	13.8
				Average	13.8

[a] Other parameters taken from Tables in manuscript. [b] Förster distance [c] Rate for electronic energy transfer assuming R = 11.95 Å. [d] Rate for electronic energy transfer assuming R = 20.1Å. [e] Rate for electronic energy transfer assuming R = 16.0Å. (see below). [f] Calculated distance over which EET is transferred using Equation 1 and experimental k_{EET} values:

$$R = \frac{R_o}{(k_{EET}\tau_D)^{1/6}} \quad \text{(Eq.1)}$$

The calculated distance R is situated in between the pyrene and thiophene unit, which is reasonable considering that the exciplex-like state comprises $(pyr^{\delta+}\text{--}thio^{\delta-})^*$.

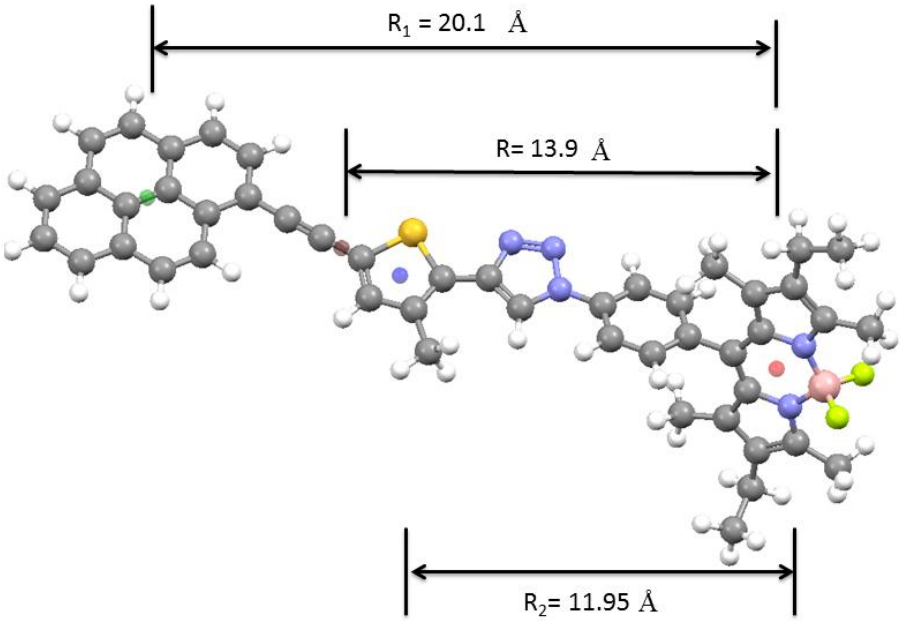

Average (R_1, R_2) = 16.0 Å

Figure 1. Computer calculated structure for **PTTBD** and selected intramolecular distances.